**ORIGINAL PAPER**

# A glassy carbon electrode modified with a nanocomposite prepared from Pd/Al layered double hydroxide and carboxymethyl cellulose for voltammetric sensing of hydrogen peroxide

Gozal Fazli [1] · Sedigheh Esmaeilzadeh Bahabadi [1] · Laleh Adlnasab [2] · Hamid Ahmar [3]

## Abstract

A Pd/Al layered double hydroxide/carboxymethyl cellulose nanocomposite (CMC@Pd/Al-LDH) was fabricated using carboxymethyl cellulose as a green substrate via co-precipitation method. The synthesized nanocomposite was characterized using different methods such as scanning electron microscopy, energy-dispersive X-ray spectroscopy, X-ray powder diffraction, transmission electron microscopy, and electrochemical techniques. A glassy carbon electrode (GCE) was then modified with the suspended composite to obtain an electrochemical sensor for hydrogen peroxide ($H_2O_2$). The voltammetric (cathodic) current of the modified GCE was measured at −380 mV (vs. Ag/AgCl), at the scan rate of 50 mV.s$^{-1}$. Results show a linear dynamic range of 1 to 120 μM, and a 0.3 μM limit of detection (at S/$N$ = 3). Intraday and interday relative standard deviations are in the ranges of 4.9–5.4% and 6.8–7.3%, respectively. The sensor was applied for the determination of $H_2O_2$ in basil extracts, milk, and spiked river water samples. The recoveries are between 96.60 and 102.30%.

**Keywords** $H_2O_2$ · Electrochemical sensor · Co-precipitation synthesis · Modified electrode · Electro-catalytic reduction · Basil extract · Milk sample · Differential pulse voltammetry · Optimization

## Introduction

Due to powerful oxidizing, sporicidal, and bactericidal characteristics, hydrogen peroxide ($H_2O_2$) has attracted great attention in different industries [1]. It is a major by-product of many enzyme based catalyzed biochemical processes through super oxide dismutase, cholesterol oxidase, urease, glucose oxidase, and horseradish peroxidase [2]. In addition, the excessive ingestion of $H_2O_2$ can result in vomiting, dizziness, and nausea in human beings. Furthermore, $H_2O_2$, accumulated in the atmosphere and water supplies, can give rise to the formation of $H_2SO_4$ and $HNO_3$, and consequently, pH of water resources decreases [3]. Additionally, Food and Drug Administration (FDA) and Occupational Safety and Health Administration (OSHA) have set the concentration level limit of $H_2O_2$ as an anti-microbial agent to be 120 ppm for vegetables, and fruits and exposure limit for human beings to be 1 ppm/1.4 mg.m$^{-3}$ in a time-weighted average scale [4].

A number of methods such as fluorescence [5], chemiluminescence [6, 7], colorimetric [8, 9] and, electrochemistry [10, 11] have been reported for this purpose. Among these reported approaches, electrochemical methods are especially promising due to their easy operation, and fabrication routes, fast analysis time, low cost, and high sensitivity [10].

✉ Sedigheh Esmaeilzadeh Bahabadi
shirin1982@gmail.com; esmaeilzadeh@uoz.ac.ir

1 Department of Biology, Faculty of Science, University of Zabol, P.O. Box, 98615-538, Zabol, Iran

2 Department of Chemistry, Chemistry and Petrochemistry Research Center, Standard Research Institute, P.O. Box, 31745-139, Karaj, Iran

3 Department of Chemistry, Faculty of Science, University of Zabol, P.O. Box, 98615-538, Zabol, Iran

Some electrochemical sensors have been reported for detection of $H_2O_2$ in different real samples [12]. These electrochemical strategies are mostly on the basis of biorecognition elements such as enzymes or proteins that lack reproducibility and thermal and chemical stability in addition to complicated fabrication method [12, 13]. To solve these problems, we have decided to develop an enzyme-free $H_2O_2$ electrochemical sensor with high sensitivity, and low limit of detection. These kinds of biosensors are on the basis of the direct reduction of $H_2O_2$ at the surface of electrodes, modified with appropriate electrocatalysts. In other words, the electrochemical signals on the surface of the bare electrodes can be improved by modification of their surfaces.

Layered double hydroxides (LDHs), mostly known as synthetic anionic clays, comprise a layered structure of positively charged metal brucite-like sheets, containing interlayer charge balancing anions, and water molecules [14]. Due to the capability of these host guest hybrid frameworks, LDHs have attracted enormous attention in different areas of research such as catalysts, adsorbents, photochemistry, ion exchanger materials, and electrode modifiers [15]. In particular, the LDH based electrochemical sensors have demonstrated exceptional catalytic performance with the advantages of being carrier for the immobilization of biological materials, nontoxicity, high stability, high sensitivity, and low Michaelis–Menten constant [16].

Using of stabilizers or supports in preparation of nanocomposites is helpful in order to control the size, morphology, and physicochemical properties of the nanoparticles such as hydrophilicity, and reactivity. Cellulose in the crystalline form with nanoscale dimensions is one of the most abundant renewable polysaccharides, which it is available on the earth [3, 17]. This biopolymer has various applicable properties like large surface area, low cost, high chemical purity, and good hydrophilicity [17, 18]. Carboxymethyl cellulose (CMC), a member of cellulose family, containing polysaccharides with high water solubility, is composed of hydroxyl, and carboxylate functional groups that are used to immobilize different materials in the field of analytical chemistry [18, 19]. Some papers have been reported in the area of electrochemical sensors, based on cellulose in different biological and environmental samples [17, 20].

Here, we report the development of a $H_2O_2$ sensor, based on a combination of Pd/Al layered double hydroxide and carboxymethyl cellulose nanocomposite (CMC@Pd/Al-LDH) modified glassy carbon electrode in the water, milk and basil extract samples. Various parameters, affecting CMC@Pd/Al-LDH/GCE performance, were studied and optimized by the cyclic voltammetry and differential pulse voltammetry methods.

# Experimental

## Chemicals

$H_2O_2$, $PdCl_2$, $Al(NO_3)_3.9H_2O$, carboxymethyl cellulose (CMC), trichloroacetic acid, citric acid, HCl, NaOH, ascorbic acid, uric acid, tannic acid, glucose monohydrate, L-cysteine, potassium hydrogen phosphate, potassium dihydrogen phosphate, and other reagents purchased from Aldrich (https://www.sigmaaldrich.com/european-export.html/) and Merck (https://www.merck.com/ index.html/), were analytical grade and were used without further purification. Working and stock solutions were daily prepared with double distilled water.

## Apparatus

To study the composition and structure of the nanocomposites, they were characterized and studied by X-ray diffraction method with a Bruker D8/advance X-ray diffraction (The Netherlands, https://www.bruker.com) with Cu-K radiation. Transmission electron microscopy (TEM) images were taken using a LEO 912AB electron microscope. Also, scanning electron microscopy (SEM), energy-dispersive X-ray spectroscopy (EDS), and EDS mapping analyses were performed using a field emission scanning electron microscope (Philips XL-30 operating at 17 kV. https://cemas.osu.edu/) to confirm surface uniformity, and composition. All electrochemical measurements were carried out using a computer controlled Sama 500 potentiostat/galvanostat (Isfahan, Iran). All electrochemical studies were accomplished on a conventional three-electrode electrochemical cell which is consisted of a glassy carbon electrode (GCE) as working electrode, an Ag/AgCl (saturated) as a reference electrode, and a platinum wire as a counter electrode. All electrodes were supplied by Azar Electrode Co. (Urmia, Iran, http://azarelectrode.ir/). Ultrasonic bath (EUROSONIC®4D, https://prosystem.euronda.com/) was used for dispersion of materials in solvents. Measurements of pH were carried out using a digital pH-meter (Ion Analyzer 827, Metrohm, https://www.metrohm.com/). The desired temperatures were obtained using a hot water bath, heated by a Heidolph heater-stirrer (Germany, https://heidolph-instruments.com/).

## Synthesis of CMC@Pd/Al-LDH

The CMC@Pd/Al-LDH was synthesized as following: Firstly, 0.5 g of carboxymethyl cellulose (CMC) was ultrasonically dispersed into 60 mL of deionized water for 15 min at 70 °C in order to be completely dissolved. Then, pH of the solution was adjusted at 9.5–10 range by 1 mol.L$^{-1}$ of NaOH solution under stirring. Then, another solution, containing 50 mL of deionized and boiling water (without $CO_2$), 0.53 g of $PdCl_2$ (3 mmol), and 0.75 g of $Al(NO_3)_3.9H_2O$ (2 mmol)

were dissolved and added dropwise to the above mentioned solution in which pH of the solution was adjusted at 9.5–10. After these steps, the resulting slurry was stirred at 70 °C for 24 h in an oil bath under vigorous stirring. Then, this solution was refluxed at 70 °C for 12 h in an oil bath without stirring as ageing step. Finally, the black solid, CMC@Pd/Al-LDH, was collected by centrifugation at 6000 rpm (RCF: 3024 g) for 15 min, rinsed with deionized water several times, and dried at 50 °C overnight.

## Preparation of CMC@Pd/Al-LDH modified glassy carbon electrode (CMC@Pd/Al-LDH/GCE)

Modifier suspension was obtained with dispersion of 5 mg of CMC@Fe/Cu-LDH in 10 mL DMF which was followed by ultrasonic agitation of mixture to obtain a stable suspension. Then, 5 μL of the suspension of CMC@Fe/Cu-LDH was accumulated on the glassy carbon electrode surface, polished by alumina and then let the modified electrode be dried at ambient condition.

## Cyclic voltammetry at CMC@Pd/Al-LDH/GCE

The CMC@Pd/Al-LDH/GCE was firstly conditioned by cyclic voltammetric cycles in the potential range of +0.5 to −1.0 V as long as stable results were obtained. In the next step, electro-reduction of $H_2O_2$ was performed on the surface of electrode with the same experimental conditions. To compare electrodes, the results of bare GCE were studied with the same procedure.

## Standard solutions and real samples preparation

Stock solution of $H_2O_2$ (2 mM) was prepared in water and stored at 4 °C. Working solutions were daily made by dilution of a certain amount of the stock solution. River water and pasteurized milk samples were obtained from Hirmand River (Zabol, Iran) and local market (Zabol, Iran), respectively. It should be mentioned that for removing all suspended materials, all real samples were centrifuged for 15 min under the rate of 3500 rpm.

For preparation of basil extract samples, four different samples were freshly collected from Zahak Basil Farms (Zabol, Iran), and they were immediately transported to the laboratory. These samples were firstly rinsed and were kept in the freezer until use. Extraction was performed according to the following method. 1 g of the basil plant was put in a crucible, placed in a solution of ice water. Then, 4 mL of trichloroacetic acid solution (10% $w/v$) was added and grinded as long as a homogenized sample was obtained. In the next step, the resulting suspension was centrifuged in the rate of 6000 rpm for 15 min. After centrifugation, the supernatant was collected; its pH was adjusted to 7.0, and was used for further electrochemical analyses.

## Results and discussion

To evaluate the morphological feature of the synthesized CMC@Pd/Al-LDH, scanning electron microscopy (SEM) images were recorded. Figure 1 shows the layers of Pd/Al-LDH with sheet-like morphology which has been formed and distributed on the surface of CMC substrate.

For more clarification, Energy-dispersive X-ray spectroscopy (EDS) was performed (Fig. S1). As can be seen, EDS analysis approves the presence of palladium and aluminum elements in the nanocomposite structure.

In addition, in order to investigate the distribution of palladium and aluminum elements in the nanocomposite structure,



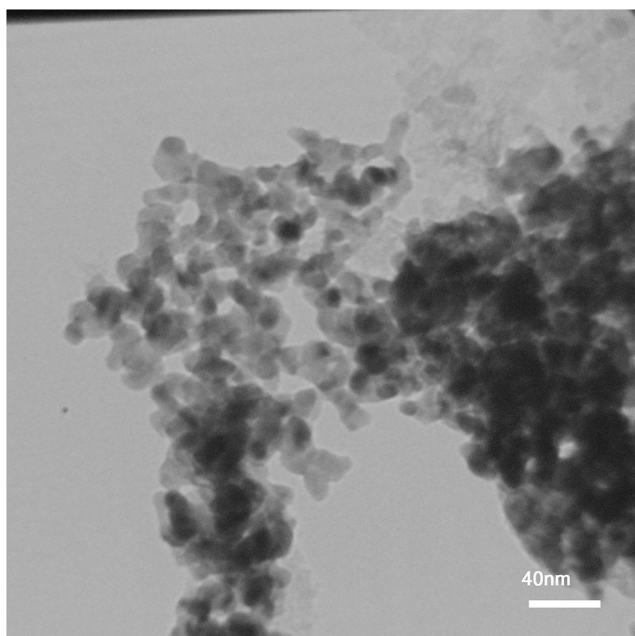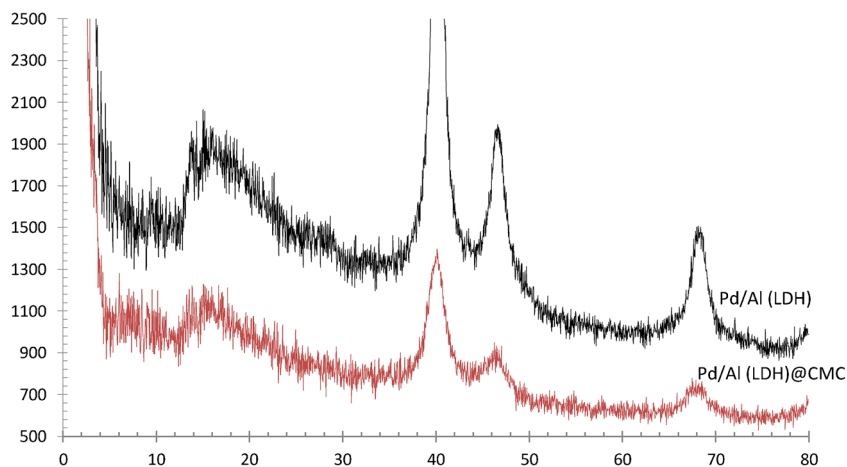**Fig. 1** FESEM image of CMC@Pd/Al-LDH
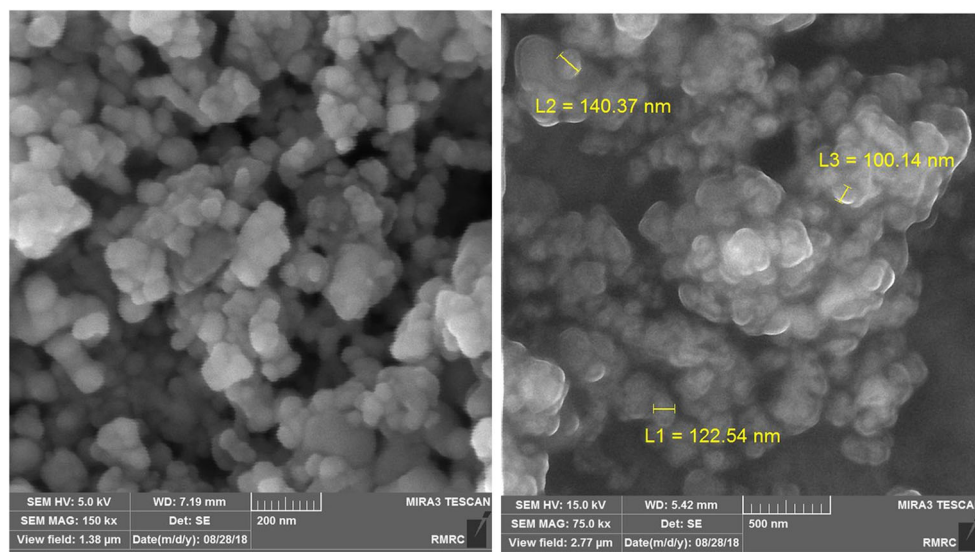
Fig. 2 TEM image of CMC@Pd/Al-LDH

EDS mapping analysis was carried out in a specific area. As can be seen in Fig. S2, the Al and Pd elements have been uniformly distributed through the nanocomposite structure.

The morphology of the CMC@Pd/Al-LDH was also investigated by transmission electron microscopy (TEM). The TEM study (Fig. 2) also confirmed the sheet-like structure of Pd/Al-LDH at CMC@Pd/Al-LDH.

Finally, the XRD patterns of Pd/Al-LDH and CMC@Pd/Al-LDH were recorded and were shown in Fig. 3. The XRD patterns show the four characteristic diffraction peaks at $2\theta = 15°$, $40°$, $46°$, and $68°$ for both Pd/Al-LDH, and CMC@Pd/Al-LDH. The typical peak at $(2\theta)$ $15°$ can be ascribed to the hydrotalcite-type structure of LDH. After modification of LDH structure with CMC, the mentioned reflection peaks equally appeared, confirming successful synthesis of CMC@Pd/Al-LDH nanocomposite.

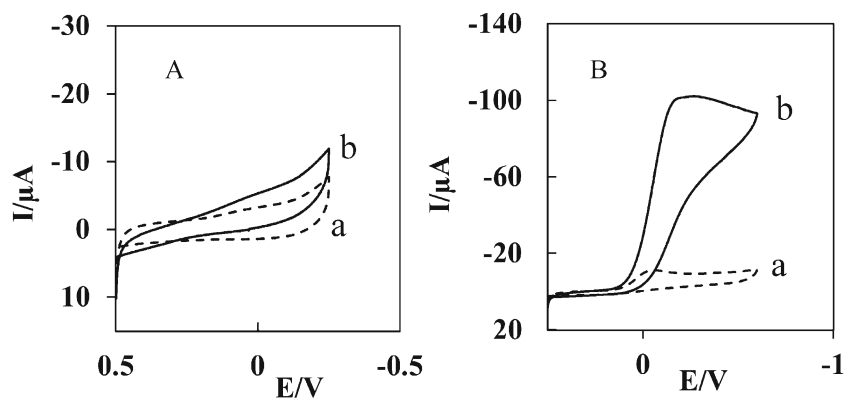# Voltammetric behavior of $H_2O_2$ on CMC@Pd/Al-LDH/GCE

## Electrochemical characterization of $H_2O_2$ on CMC@Pd/Al-LDH/GCE

In the next experiments, the electrochemical reduction of $H_2O_2$ on the both modified and unmodified electrodes was investigated in the presence and absence of $H_2O_2$ (Fig. 4). As can be seen, the bare GCE exhibits a negligible signal for $H_2O_2$ reduction. However, the CMC@Pd/Al-LDH/GCE exhibits a considerable increase in the reduction peak of $H_2O_2$. The increase in the electrochemical sensitivity of the hybrid of CMC and Pd/Al-LDH can be due to the different reasons. First and foremost, large quantities of Pd/Al-LDH can be successfully dispersed on the surface of CMC, providing more available sites for electrochemical reactions. Apart from this, the Pd/Al-LDH substrate can speed up the electrochemical processes by confining $H_2O_2$ inside the modifier and/or near the electrode surface. Therefore, these results show that reduction of $H_2O_2$ can be electrocatalyzed by combination of properties of Pd/Al layered double hydroxide and carboxymethyl cellulose.

## Influence of pH

Electrochemical behavior of $H_2O_2$ depends on the pH of electrolyte solution [1]. Therefore, the effect of various pH values on the determination of $H_2O_2$ using CMC@Pd/Al-LDH/GCE was studied and optimized in the range of 4.0 to 9.0 by CV method. As can be seen in Fig. S3, the reduction peak currents rose as the pH increased gradually from 4.0 to 7.0 which were followed by a slight decrease in the pH range from 7.0 to 9.0. On the other hand, maximum efficiency of CMC@Pd/Al-LDH/GCE towards reduction of $H_2O_2$ was obtained

Fig. 3 XRD spectrum of Pd/Al-LDH and CMC@Pd/Al-LDH

**Fig. 4** The CV responses of (A) blank solution and (B) 50 μM $H_2O_2$ on (**a**) bare GCE, and (**b**) CMC@Pd/Al-LDH/GCE in 0.1 M phosphate buffer (pH 7.0) at 50 mV.s$^{-1}$ scan rate
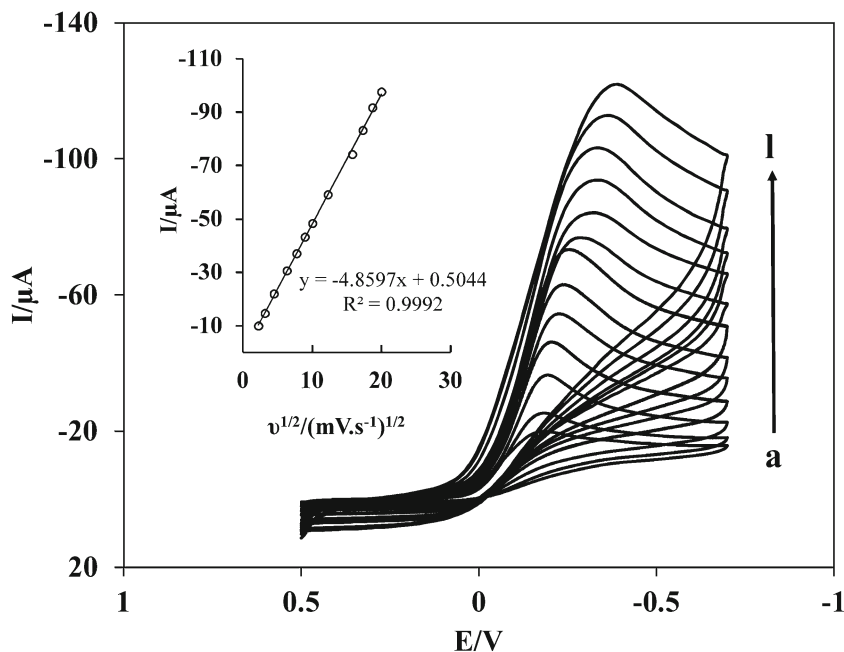


in pH 7.0 Therefore, pH of 7.0 was chosen for subsequent experiments.

## Effect of scan rate on the voltammetric behavior of $H_2O_2$ at CMC@Pd/Al-LDH/GCE

Effect of scan rate was also studied to evaluate the mechanism of electrochemical reaction on the electrode surface. To perform this, cyclic voltammograms were recorded on CMC@Pd/Al-LDH/GCE in the presence of 50 μM $H_2O_2$ at different scan rates in the range of 5 to 400 mV.s$^{-1}$. As can be seen in the Fig. 5 inset, peak currents depend on the square root of scan rate. This reveals that electrochemical reaction of $H_2O_2$ on the CMC@Pd/Al-LDH/GCE surface is controlled by diffusion mechanism according to following equation:

$$I_P = -4.8597 \, v^{1/2} + 0.5044 \, \left(R^2 = 0.9992\right)$$

Furthermore, the reduction peak potentials are shifted toward more negative values which are expected for an irreversible electrode reaction [21].

## Electrochemical determination of $H_2O_2$

To test the applicability of the CMC@Pd/Al-LDH/GCE for the $H_2O_2$ detection, the electrochemical peak responses were investigated as a function of $H_2O_2$ concentration (Fig. 6). The sensor indicates two linear dynamic ranges of 1–50 μM ($R^2 = 0.9986$) and 50–120 μM ($R^2 = 0.9981$). Also, limit of detection was calculated to be 0.3 μM, based on signal to noise of 3.

To test the intraday repeatability of the method, DPVs were recorded in five repetitive experiments in different concentrations of $H_2O_2$ (Table S1). RSDs of ≤5.4% were obtained at all concentrations, indicating high precision in the results of the sensor. In order to

**Fig. 5** The CV responses of 50 μM $H_2O_2$ on CMC@Pd/Al-LDH/GCE in 0.1 M phosphate buffer (pH 7.0) at various scan rates (a-l: 5, 10, 20, 40, 60, 80, 100, 150, 250, 300, 350, and 400 mV.s$^{-1}$). Inset: plot of the peak current versus the square root of scan rate

**Fig. 6** The DPV responses of CMC@Pd/Al-LDH/GCE in 0.1 M phosphate buffer at pH 7.0 with different concentrations of $H_2O_2$ (0–120 μM) at the scan rate of 50 mV.s$^{-1}$. Inset: plot of the peak current versus concentration of $H_2O_2$ at −380 mV vs. Ag/AgCl
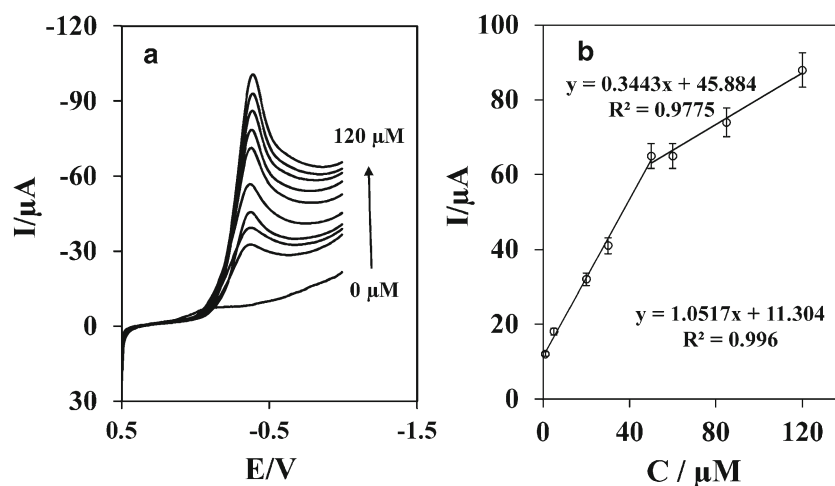


evaluate the interday repeatability, five replicates in 5 days were performed in three concentration levels of $H_2O_2$. Relative standard deviations of 6.8–7.3% confirm acceptable precision of the method.

In addition, to study the stability of the sensor, the CMC@Pd/Al-LDH/GCE was stored at room temperature and analyses were carried out in different time periods within 10 days. The results show that 93.2% of initial current can be obtained at end of this period, illustrating that the CMC@Pd/Al-LDH/GCE has an excellent stability.

The selectivity of the developed sensor was investigated in order to confirm its practical application in $H_2O_2$ determination. Therefore, the effect of several possible interfering substances such as ascorbic acid, uric acid, tannic acid, glucose, L-cysteine, $NO_3^-$, $Mg^{2+}$, $Ca^{2+}$, and $Zn^{2+}$ were investigated using DPV method. The results show that the addition of 50 μM $H_2O_2$ brought about an evident response current while there is no significant change in current in the presence of other substances at the same concentration. These results suggest that CMC@Pd/Al-LDH/GCE has a good selectivity for $H_2O_2$ reduction and the coexistence of these interfering species did not affect $H_2O_2$ quantification.

**Table 1**    Determination of $H_2O_2$ in real samples

| Sample | Spiked (μM) | Found (μM) | RSD (%, $n = 3$) | Recovery (%) |
|---|---|---|---|---|
| River water 1 | 50 | 51.15 | 4.8 | 102.30 |
| River water 2 | 80 | 78.45 | 4.6 | 98.06 |
| Milk sample 1 | 5 | 4.97 | 5.2 | 99.40 |
| Milk sample 2 | 20 | 19.65 | 4.6 | 98.25 |
| Basil extract 1 | 10 | 9.66 | 4.8 | 96.60 |
| Basil extract 2 | 60 | 59.12 | 5.1 | 98.54 |

## Real sample analysis

In order to evaluate the practical use of the CMC@Pd/Al-LDH/GCE in the real samples, recovery tests were performed by determination of $H_2O_2$ in different media such as river water, pasteurized milk (diluted 100-fold with phosphate buffer solution, 0.1 M, pH 7.0), and basil extract samples. As shown in Table 1, the recoveries were obtained to be in the range of 96.60–102.30%, indicating that the CMC@Pd/Al-LDH/GCE is suitable for analysis of $H_2O_2$ in real samples, and there is no significant matrix effect in the analysis of $H_2O_2$ by this sensor.

Finally, Table 2 compares some figures of merits of previously reported electrochemical sensors for quantification of hydrogen peroxide with those of the CMC@Pd/Al-LDH/GCE [22–38]. The electrode assembled in this work performs as well as other works or somewhat better in terms of detection limit and linear dynamic range. Among the works of Table 2, using myoglobin/Salep- combined with mesoporous carbon foam shows much lower LOD than that of the proposed electrode. But this sensor tends to be more complex in design compared to the CMC@Pd/Al-LDH/GCE. The graphene and gold nanorods modified glassy carbon electrode [25] have also excellent sensing properties such as high sensitivity and wide linear range, but its fabrication procedure is more complex and requires expensive materials.

## Conclusion

In the present research, the CMC@Pd/Al-LDH was synthesized and used to develop an electrochemical sensor for $H_2O_2$ determination. The CMC@Pd/Al-LDH/GCE exhibited higher sensitivity and lower limit of detection in comparison with those of

**Table 2**   A comparison between the CMC@Pd/Al-LDH/GCE and some other sensors for the determination of $H_2O_2$

| Electrode | Method | LOD ($\mu M$) | LR (mM) | Sensitivity ($\mu A\ mM^{-1}\ cm^{-2}$) | Reference |
|---|---|---|---|---|---|
| FcAPS/GCE[a] | Amperometry | 2.07 | 10–10,000 | 0.05 | [22] |
| MWCNT/AgNPs/GCE[b] | Amperometry | 0.5 | 50–17,000 | 1.42 | [23] |
| GS@CeO$_2$/Au/GCE[c] | Cyclic voltammetry | 0.26 | 1–10,000 | – | [24] |
| GR-AuNRs/GCE[d] | Amperometry | 10 | 30–5000 | 389.2 | [25] |
| Fe$_3$O$_4$/Au/HRP/GS/SPCE[e] | Amperometry | 12 | 20–2500 | – | [26] |
| MnOOH/GCE[f] | Cyclic voltammetry | 115 | 150–1600 | – | [27] |
| Hollow CuO$_x$/NiO$_y$ nanocomposite/GCE | amperometry Cyclic voltammetry | 0.09 | 0.0003–9.0 | 271.1 | [28] |
| type Fe$_3$O$_4$@Au-PB[g] | Cyclic voltammetry | 1.1 | – | – | [29] |
| GDC[h]-NiO modified electrodes | Cyclic voltammetry and amprometry | 0.0015 | 0.00001–0.0039 | 107.22 | [30] |
| hollow urchin-like $\alpha$-MnO$_2$/ GCE | Cyclic voltammetry | 0.08 | 0.00024–0.1 | 0.55 | [31] |
| carbonized ZIF@rGO particles[i] | Cyclic voltammetry - chronoamperometry | 3.3 | 0.005–0.02 | 0.272 | [32] |
| GO-PAMAM-Fe$^{2+}$ and PANI[j] | DPV | 0.18 | 0.0005–2 | 2.71 | [33] |
| Pt-Pd/MoS$_2$/GCE | Cyclic voltammetry | 3.4 | 0.01–0.08 | 7.64 | [34] |
| N-CNFht[k]/GCE | Amprometry | 0.62 | 0.01–0.71 | 357 | [35] |
| NH-CDs-HRP[l] | Cyclic voltammetry | 0.0018 | 0.000005–0.00059 | 145 | [36] |
| Mb/S- MCF/GCE[m] | Cyclic voltammetry | 0.18 | 0.001–0.08 | 2.2 | [37] |
| Cu$_2$O/PANI/rGO[n] | Cyclic voltammetry | 0.5 | 0.0008–12.78 | 39.4 | [38] |
| CMC@Pd/Al-LDH | DPV | 0.3 | 0.001–0.12 | 16.27 | This work |

[a] Ferrocene carboxylic acid entrapped in cross-linked amino-polyethersulfone film/glassy carbon electrode. [b] Multi-wall carbon nanotube/silver nanoparticle nanohybrids modified gold electrode. [c] Gold nanoparticles loaded on ongraphene sheets@cerium oxide nanocomposites modified gold electrode. [d] Graphene and gold nanorods modified glassy carbon electrode. [e] Fe$_3$O$_4$–Au magnetic nanoparticles coated horseradish peroxidase (HRP) and graphene sheets (GS)–Nafion film modified screen-printed carbon electrode (SPCE). [f] MnOOH nanowire composite film modified glass carbon electrode. [g] magnetic core/dual-functional-shell nanocomposites composed of magnetite, gold and Prussian blue. [h] glucose derived sheet-like carbons. [i] carbonized zeolitic imidazolate frameworks/reduced graphene oxide. [j] Graphene oxide/poly(amidoamine) dendrimer- Polyaniline. [k] Nitrogen-doped carbon nanofibers. [l] Horseradish peroxidase- amino functionalized carbon dots. [m] myoglobin/Salep-Mesoporous carbon foam/glassy carbon electrode. [n] Cuprous oxide/polyaniline/reduced graphene oxide

bare GCE, and many of previously reported researches. The increase in the electrochemical results can be related to the more available sites for electrochemical reactions, confinement of $H_2O_2$ inside the modifier and/or near the electrode surface in addition to increase in the specific surface area by CMC. Taking all this into account, the sensor can be a very sensitive and promising device for the development of an enzyme free $H_2O_2$ sensor in the future. Finally, this work introduces a new approach to immobilize two different materials such as Pd/Al-LDH with specific electrochemical properties, and CMC with high specific surface area on the electrode surface with the aim of electroanalysis and biosensing applications.

## Compliance with ethical standards

**Conflict of interest**   The author(s) declare that they have no competing interests.

# References

1. Benvidi A, Nafar MT, Jahanbani S, Tezerjani MD, Rezaeinasab M, Dalirnasab S (2017) Developing an electrochemical sensor based on a carbon paste electrode modified with nano-composite of reduced graphene oxide and CuFe$_2$O$_4$ nanoparticles for determination of hydrogen peroxide. Mater Sci Eng C 75:1435–1447
2. Bian X, Guo K, Liao L, Xiao J, Kong J, Ji C, Liu B (2012) Nanocomposites of palladium nanoparticle-loaded mesoporous carbon nanospheres for the electrochemical determination of hydrogen peroxide. Talanta 99:256–261
3. Li Q, Gao W, Zhang X, Liu H, Dou Li G, Li Y, Wang Z, Liu H (2017) Green synthesis of palladium nanoparticles with carboxymethyl cellulose for degradation of azo-dyes. Mater Chem Phys 187:133–140
4. Devasenathipathy R, Liu YX, Yang C, Wang SF (2017) Simple electrochemical growth of copper nanoparticles decorated silver nanoleaves for the sensitive determination of hydrogen peroxide in clinical lens cleaning solutions. Sensors Actuators B Chem 252:862–869
5. Gao C, Tian Y, Zhang R, Jing J, Zhang X (2017) Endoplasmic reticulum-directed ratiometric fluorescent probe for quantitive detection of basal $H_2O_2$. Anal Chem 89:12945–12950

6. Ding H, Tang Z, Zhang L, Dong Y (2019) Electrogenerated chemiluminescence of black phosphorus nanosheets and its application in the detection of $H_2O_2$. Analyst 144:1326–1333

7. Xie JX, Chen WJ, Wu XX, Wu YY, Lin H (2017) Enhanced luminol chemiluminescence by co–Fe LDH nanoplates and its application in $H_2O_2$ and glucose detection. Anal Methods 9:974–979

8. Cui M, Zhou J, Zhao Y, Song Q (2017) Facile synthesis of iridium nanoparticles with superior peroxidase-like activity for colorimetric determination of $H_2O_2$ and xanthine. Sensors Actuators B Chem 243:203–210

9. Wang Y, Zhang D, Wang J (2018) Metastable $\alpha$-AgVO$_3$ microrods as peroxidase mimetics for colorimetric determination of H2O2. Microchim Acta 185(1):1–8

10. Rui Q, Komori K, Tian Y, Liu H, Luo Y, Sakai Y (2010) Electrochemical biosensor for the detection of H2O2 from living cancer cells based on ZnO nanosheets. Anal Chim Acta 670:57–62

11. Chen W, Cai S, Ren QQ, Wen W, Zhao YD (2012) Recent advances in electrochemical sensing for hydrogen peroxide: a review. Analyst 137:49–58

12. Ensafi AA, Abarghoui MM, Rezaei B (2014) Electrochemical determination of hydrogen peroxide using copper/porous silicon based non-enzymatic sensor. Sensors Actuators B Chem 196:398–405

13. Periasamy AP, Ho YH, Chen SM (2011) Multiwalled carbon nanotubes dispersed in carminic acid for the development of catalase based biosensor for selective amperometric determination of $H_2O_2$ and iodate. Biosens Bioelectron 29:151–158

14. Chen H, Hu L, Chen M, Yan Y, Wu L (2014) Nickel–cobalt layered double hydroxide Nanosheets for high-performance Supercapacitor electrode materials. Adv Funct Mater 24:934–942

15. Mishra G, Dash B, Pandey S (2018) Layered double hydroxides: a brief review from fundamentals to application as evolving biomaterials. Appl Clay Sci 153:172–186

16. Li M, Zhu JE, Zhang L, Chen X, Zhang H, Zhang F, Xu S, Evans DG (2011) Facile synthesis of NiAl-layered double hydroxide/graphene hybrid with enhanced electrochemical properties for detection of dopamine. Nanoscale 3:4240–4246

17. Sprick C, Chede S, Oyanedel-Craver V, Escobar IC (2018) Bio-inspired immobilization of casein-coated silver nanoparticles on cellulose acetate membranes for biofouling control. J Environ Chem Eng 6:2480–2491

18. Ahmar H, Keshipour S, Hosseini H, Fakhari AR, Shaabani A, Bagheri A (2013) Electrocatalytic oxidation of hydrazine at glassy carbon electrode modified with ethylenediamine cellulose immobilized palladium nanoparticles. J Electroanal Chem 690:96–103

19. Lang X, Xing-Cai W, Jun-Jie Z (2008) Green preparation and catalytic application of Pd nanoparticles. Nanotechnology 19:1–6

20. Palanisamy S, Velusamy V, Ramaraj S, Chen SW, Yang TCK, Balu S, Banks CE (2019) Facile synthesis of cellulose microfibers supported palladium nanospindles on graphene oxide for selective detection of dopamine in pharmaceutical and biological samples. Mater Sci Eng C 98:256–265

21. Razmi H, Mohammad-Rezaei R, Heidari H (2009) Self-prussian blue nanoparticles based electrochemical sensor for high sensitive determination of $H_2O_2$ in acidic media. Electroanalysis 21:2355–2362

22. Mattoussi M, Matoussi F, Raouafi N (2018) Non-enzymatic amperometric sensor for hydrogen peroxide detection based on a ferrocene-containing cross-linked redox-active polymer. Sensors Actuators B Chem 274:412–418

23. Zhao W, Wang H, Qin X, Wang X, Zhao Z, Miao Z et al (2009) A novel nonenzymatic hydrogen peroxide sensor based on multi-wall carbon nanotube/silver nanoparticle nanohybrids modified gold electrode. Talanta 80:1029–1033

24. Yang X, Ouyang Y, Wu F, Hu Y, Ji Y, Wu Z (2017) Size controllable preparation of gold nanoparticles loading on graphene sheets@ cerium oxide nanocomposites modified gold electrode for nonenzymatic hydrogen peroxide detection. Sensors Actuators B Chem 238:40–47

25. Pang P, Yang Z, Xiao S, Xie J, Zhang Y, Gao Y (2014) Nonenzymatic amperometric determination of hydrogen peroxide by graphene and gold nanorods nanocomposite modified electrode. J Electroanal Chem 727:27–33

26. Xin Y, Fu-bing X, Hong-wei L, Feng W, Di-zhao C, Zhao-yang W (2013) A novel $H_2O_2$ biosensor based on Fe$_3$O$_4$–au magnetic nanoparticles coated horseradish peroxidase and graphene sheets–Nafion film modified screen-printed carbon electrode. Electrochim Acta 109:750–755

27. Cao X, Wang N, Wang L, Mo C, Xu Y, Cai X, Guo L (2010) A novel non-enzymatic hydrogen peroxide biosensor based on ultralong manganite MnOOH nanowires. Sensors Actuators B Chem 147:730–734

28. Long L, Liu X, Chen L, Li D, Jia J (2019) A hollow CuOx/NiOy nanocomposite for amperometric and non-enzymatic sensing of glucose and hydrogen peroxide. Microchim Acta 186:74–84

29. Li Y, Liu J, Fu Y, Xie Q, Li Y (2019) Magnetic-core@dual-functional-shell nanocomposites with peroxidase mimicking properties for use in colorimetric and electrochemical sensing of hydrogen peroxide. Microchim Acta 186:456–464

30. Sivakumar M, Veeramani V, Chen SM, Madhu R, Liu SB (2019) Porous carbon-NiO nanocomposites for amperometric detection of hydrazine and hydrogen peroxide. Microchim Acta 186:59–66

31. Song H, Zhao H, Zhang X, Xu Y, Cheng X, Gao S, Huo L (2019) A hollow urchin-like $\alpha$-MnO2 as an electrochemical sensor for hydrogen peroxide and dopamine with high selectivity and sensitivity. Microchim Acta 186:210–221

32. Li Z, Jiang Y, Wang Z, Wang W, Yuan Y, Wu X., ... & Wang D (2018) Nitrogen-rich core-shell structured particles consisting of carbonized zeolitic imidazolate frameworks and reduced graphene oxide for amperometric determination of hydrogen peroxide. Microchim Acta 185:501–509.

33. Tang J, Huang L, Cheng Y, Zhuang J, Li P, Tang D (2018) Nonenzymatic sensing of hydrogen peroxide using a glassy carbon electrode modified with graphene oxide, a polyamidoamine dendrimer, and with polyaniline deposited by the Fenton reaction. Microchim Acta 185:569–577

34. Sha R, Vishnu N, Badhulika S (2018) Bimetallic Pt-Pd nanostructures supported on MoS2 as an ultra-high performance electrocatalyst for methanol oxidation and nonenzymatic determination of hydrogen peroxide. Microchim Acta 185:399–409

35. Lyu YP, Wu YS, Wang TP, Lee CL, Chung MY, Lo CT (2018) Hydrothermal and plasma nitrided electrospun carbon nanofibers for amperometric sensing of hydrogen peroxide. Microchim Acta 185:371–377

36. Su Y, Zhou X, Long Y, Li W (2018) Immobilization of horseradish peroxidase on amino-functionalized carbon dots for the sensitive voltammetric detection of hydrogen peroxide. Microchim Acta 185:114–121

37. Jahanbakhshi M (2018) Myoglobin immobilized on mesoporous carbon foam in a hydrogel (selep) dispersant for voltammetric sensing of hydrogen peroxide. Microchim Acta 185:121–128

38. Liu J, Yang C, Shang Y, Zhang P, Liu J, Zheng J (2018) Preparation of a nanocomposite material consisting of cuprous oxide, polyaniline and reduced graphene oxide, and its application to the electrochemical determination of hydrogen peroxide. Microchim Acta 185:172–179

**Publisher's note** Springer Nature remains neutral with regard to jurisdictional claims in published maps and institutional affiliations.